Carbohydrate Polymers 112 (2014) 569–577

Contents lists available at ScienceDirect

Carbohydrate Polymers

journal homepage: www.elsevier.com/locate/carbpol

# Hydration and the phase diagram of acid hydrolyzed potato starch

Jonas Carlstedt[a], Joanna Wojtasz[a], Peter Fyhr[b], Vitaly Kocherbitov[a,*]

[a] Malmö University, Faculty of Health and Society, Biomedical Science, Malmö SE-205 06, Sweden
[b] Magle AB, Fjälkestadsvägen336-15, Kristianstad SE-291 94, Sweden

ARTICLE INFO

*Article history:*
Received 14 March 2014
Received in revised form 5 June 2014
Accepted 6 June 2014
Available online 21 June 2014

*Keywords:*
Glass transition
Crystallization
Sorption calorimetry
QCM-D
X-ray scattering
DSC

ABSTRACT

We investigated hydration of acid hydrolyzed potato starch (maltodextrin) employing a multi-method approach. In particular, synchrotron radiation X-ray scattering and differential scanning calorimetry were used, and, for the first time, the material was investigated with sorption calorimetry and a newly developed quartz crystal microbalance with humidity scanning. The dry starch was found to be in an amorphous state. During hydration it exhibits a glass transition in both bulk and thin film samples, followed by an exothermic event where the starch crystallized. Recrystallized bulk samples displayed neither a pronounced glass transition nor crystallization upon hydration whereas both events occurred in thin film samples. The hydration-driven crystallization resulted in an X-ray pattern consistent with the coexistence of A and B type crystallites; however, at higher water concentrations only the B form occurred. The results were used to construct the first ever acid hydrolyzed starch–water phase diagram.


## 1. Introduction

Starch is a readily available biopolymer synthesized in densely packed granules in plants for energy storage. Used in several applications in, e.g., the food, paper and packaging, and the pharmaceutical industry, starch is a carbohydrate composed of the two polysaccharides amylose and amylopectin. While amylose is essentially linear, amylopectin is highly branched with short chains organized in clusters (Buléon, Colonna, Planchot, & Ball, 1998; French, 1972). The granular organization of starch comprises alternating amorphous and semi-crystalline growth rings (Pérez & Bertoft, 2010). Native starch structure is an active research area and some of the major findings include the lamellar stacking of amylopectin double helixes in the semi-crystalline growth rings and that the amylopectin double helixes in the lamellae can be organized in various ways such as the A and B type crystallinity (Hsein-Chih & Sarko, 1978a; Hsien-Chih & Sarko, 1978b). While cereal starches preferentially show A type crystallinity, tuber starches, such as potato, show B type crystallinity.

The native form of starch is not very useful in industrial applications; however, in the presence of water, starch undergoes gelatinization upon heating. There is some debate in the literature about what the term gelatinization includes (Karapantsios, Sakonidou, & Raphaelides, 2002; Lelièvre & Liu, 1994; Vermeylen et al., 2006b), but generally it is considered the process where the starch granules swell, lose their long-order structure, and, at least partially, dissolve. Starch gelatinization has been widely studied by means of, e.g., differential scanning calorimetry (DSC), X-ray and neutron scattering techniques, and microscopy (Donovan, 1979; Jenkins & Donald, 1998; Karlsson & Eliasson, 2003; Lelièvre & Liu, 1994; Morikawa & Nishinari, 2000; Vermeylen et al., 2006a, 2006b; Waigh, Gidley, Komanshek, & Donald, 2000). After the gelatinization process, starch can undergo retrogradation upon storage below the gelatinization temperature (Karlsson & Eliasson, 2003).

Another important material property of starch is its glass transition where the molecules in the amorphous fraction of the starch transform from a frozen to a mobile state. Glass transitions of starch have been measured by, e.g., DSC (Thiewes & Steeneken, 1997), and it has been found that they are sensitive to the addition of plasticizers, i.e., small molecules such as water or glycerol, which shift the glass transition to lower temperatures (Lourdin, Coignard, Bizot, & Colonna, 1997). The presence of crystallites in the material can make the detection of the glass transition in DSC difficult since the fraction of amorphous material can be small and the step in the heat capacity thus small. It should be noted that parts of the same chain can be in a crystallite whereas another part is in a disordered state in semi-crystalline polymers (Thiewes & Steeneken, 1997).

One way of increasing the usefulness of starch for industrial applications is by treating it with acid at elevated temperature.

* Corresponding author. Tel.: +46 40 6657946.
*E-mail addresses:* jonas.carlstedt@mah.se (J. Carlstedt), joanna.wojtasz@gmail.com (J. Wojtasz), pf@magle.se (P. Fyhr), vitaly.kocherbitov@mah.se (V. Kocherbitov).

http://dx.doi.org/10.1016/j.carbpol.2014.06.037
0144-8617/

It is mainly the amorphous part of the native starch that is subjected to acid hydrolysis and the method is used as a pretreatment in various industrial applications (e.g., for gums, pastilles, jellies) to decrease viscosity and increase gel strength (Knill & Kennedy, 2005). Acid hydrolysis is also used to determine the degree of crystallinity of native starches (Buléon et al., 1998) and to prepare starch nanocrystals (Lin, Huang, Chang, Anderson, & Yu, 2011).

In the present work, we characterize mixtures of spray-dried acid hydrolyzed potato starch (maltodextrin) and water using a combination of sorption calorimetry, small- and wide-angle X-ray scattering, humidity scanning quartz crystal microbalance with dissipation monitoring, and differential scanning calorimetry. Although acid hydrolyzed starch to some extent has been characterized before, there is a lack of systematic studies. The aim of the present study is thus to investigate the hydration or temperature-induced reorganization of the material. Moreover, based on all obtained data we construct the first to our knowledge temperature–composition phase diagram of the acid hydrolyzed potato starch–water system.

## 2. Materials and methods

### 2.1. Materials

Spray-dried acid hydrolyzed potato starch (maltodextrin) was produced by Lantmännen Reppe AB (Växjö, Sweden). The mass distribution of the material was supplied by the manufacturer (Supplementary Material, Figure S1). Native potato starch was obtained from Lyckeby Starch AB (Kristianstad, Sweden).

Samples for differential scanning calorimetry (DSC) and small/wide-angle X-ray scattering were prepared either by adding water directly to dried starch or by equilibrating the dried starch in controlled relative humidity using saturated salt solutions (Greenspan, 1976). Recrystallized acid hydrolyzed starch was prepared by equilibrating the material at 97.3% RH (in the presence of a saturated $K_2SO_4$ solution) for 1 week. The material was subsequently dried in vacuum in the presence of 3 Å molecular sieves and ground in a mortar. Before use, the recrystallized starch was further dried in vacuum for 24 h at room temperature in the presence of 3 Å molecular sieves.

Completely dry material is required for sorption calorimetry experiments, i.e., the water activity and the water content should initially be zero. Therefore, after drying for 24 h in vacuum at room temperature in the presence of 3 Å molecular sieves, the sample was transferred to the sorption calorimetry cell inside a glove box with a dry atmosphere.

### 2.2. Scanning electron microscopy

The appearance of acid hydrolyzed potato starch in comparison to native starch was examined with a scanning electron microscope (Zeiss EVO LS10 SEM). The experiments were performed at 25 °C under vacuum and then at defined relative humidity. The material was dried in vacuum to ensure minimal moisture content, and deposited on a standard sample holder covered with graphite.

### 2.3. Sorption calorimetry

Hydration of starch was investigated with the sorption calorimetry method, which simultaneously measures the water activity $a_w$ and the partial molar enthalpy of mixing of water $H_w^{mix}$, also called the hydration enthalpy, as a function of water content (Wadsö & Markova, 2002). The experiments were performed at 25 °C or 40 °C in a two-chamber calorimeter cell inserted in a double-twin microcalorimeter (Wadsö & Wadsö, 1996). The dry sample is loaded into the upper (sorption) chamber whereas water is injected into the lower (vaporization) chamber of the calorimeter cell. Evaporated water diffuses through the tube connecting the two chambers and the thermal powers of the upper and lower chambers are recorded. The thermal power of evaporated water recorded in the vaporization chamber is used to calculate the water activity as described elsewhere (Kocherbitov, 2004). The partial molar enthalpy of mixing of water is calculated from the relation below:

$$H_w^{mix} = H_w^{vap} + H_w^{vap}\frac{P^{sorp}}{P^{vap}}$$

where $P^{sorp}$ and $P^{vap}$ are the recorded thermal powers in the sorption and vaporization chambers, respectively, and $H_w^{vap}$ is the molar enthalpy of vaporization of pure water (Wadsö & Markova, 2002).

### 2.4. Humidity scanning quartz crystal microbalance with dissipation (HS-QCM-D)

The quartz crystal microbalance (QCM-D) is a very sensitive technique, which allows measurements on very small amount of sample. Simultaneous measurements of changes in frequency and dissipation allows determination of mass, thickness, swelling and rheological properties of the sample at defined moments. The measurement is based on the shift in oscillation frequency caused by the application of a mass on the quartz sensor. For rigid films the Sauerbrey equation applies (Sauerbrey, 1959):

$$\frac{\Delta f}{n} = -\frac{2mf_0^2}{Z_q}$$

where $\Delta f$ is the shift in frequency, $n$ is the overtone number, $m$ is the mass in kg m$^{-2}$, $f_0$ is the fundamental frequency, and $Z_q$ is the acoustic or mechanical impedance of quartz. For viscoelastic films, additional modeling is needed to determine the mass of the sample (Johannsmann, 1999). In parallel, the rheological properties are tracked by the dissipation monitoring. The dependence of sample behavior on the water activity can be studied using a humidity module. It is built up from two chambers separated by a porous membrane that ensures permeation of water vapor but not liquids. Pumping media (e.g., nitrogen, aqueous salt solutions, water) through one of the compartments determine the relative humidity above the sample-covered sensor located in the second compartment. A novel method recently developed in our lab makes use of a continuous dilution of a saturated lithium chloride solution which results in a continuous scanning of water activity above the sample film (Graf & Kocherbitov, 2013).

For analysis of the starch system with respect to changing humidity the use of quartz crystal microbalance with dissipation monitoring (QCM-D, Q-sense E4) was combined with a Q-sense humidity module 401. AZ-cut, 5 MHz quartz sensors with silica surface (QSX 303, silicon dioxide, 50 nm, Biolin Scientific AB, Västra Frölunda, Sweden) were used. The sensor was drop-coated with the sample and placed in the humidity module; 0% relative humidity was achieved by flowing dry nitrogen through the chamber. A flow of saturated lithium chloride solution through the chamber was then started and a continuous increase of the relative humidity was ensured by dilution of the LiCl solution by water. Analysis of the result was performed in Q-soft and Q-tools (Q-sense AB) and in Matlab (The MathWorks Inc.).

### 2.5. Small/wide-angle X-ray scattering (SAXS/WAXS)

SAXS and WAXS experiments were performed at the MAX IV Laboratory, Lund, at Beamline I911-4 described elsewhere (Labrador, Cerenius, Svensson, Theodor, & Plivelic, 2013). The wavelength of the beam was 0.91 Å and the sample to detector distance was 1327 mm (SAXS) or 319.85 mm (WAXS). The software

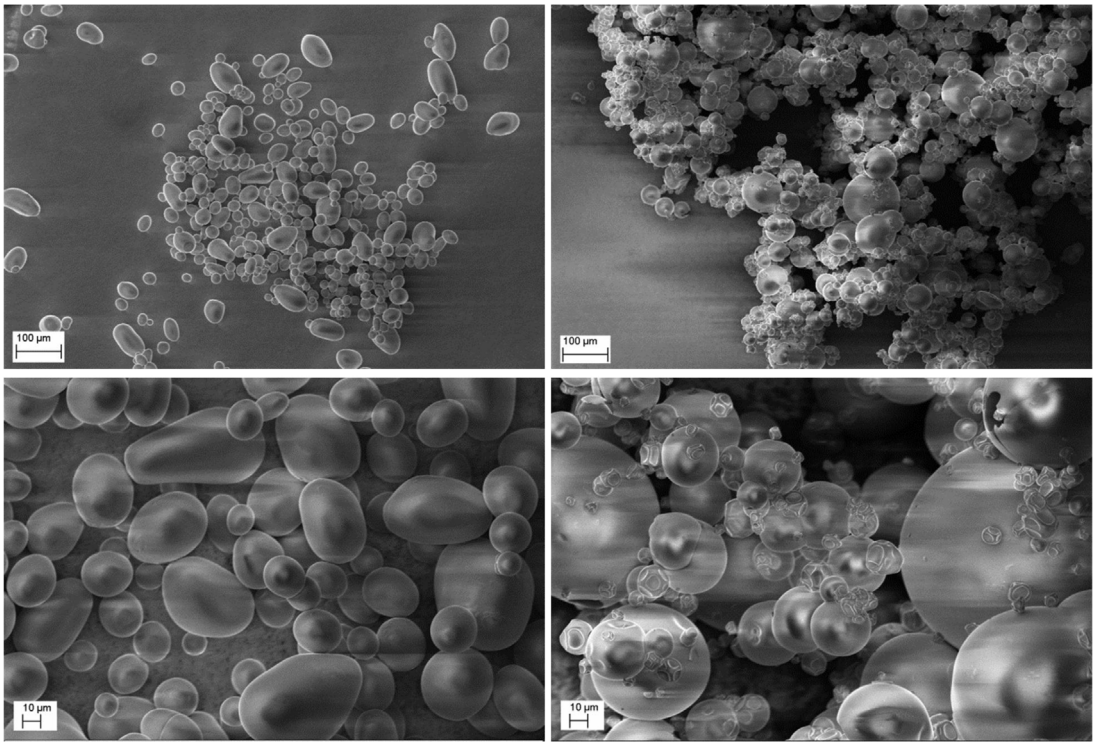


**Fig. 1.** Micrographs of native potato starch (left) and acid hydrolyzed potato starch (right) in vacuum at room temperature at two different magnifications.

Fit2d was used for data evaluation (Hammersley, 1997). Background subtraction (empty solid sample holder or capillary filled with water) was performed using programs written in Matlab.

### 2.6. Differential scanning calorimetry (DSC)

A DSC1 from Mettler Toledo was used to analyze mixtures of acid hydrolyzed starch and water. Hermetically sealed 40 µl aluminum crucibles containing the samples were cooled down to −50 °C and subsequently heated to 100 °C at a scanning rate of either 1 °C min$^{-1}$ or 10 °C min$^{-1}$. For one selected sample composition several lower scanning rates were also used in order to extrapolate the endset of melting of ice to zero scan rate. Indium was used as a calibrant and an empty aluminum crucible (40 µl) was used as a reference.

## 3. Results and discussion

The obtained spray-dried acid hydrolyzed starch was a white powder with an aqueous solubility between 1 and 2 wt% at room temperature. However, it was found that the material strikingly changed its physical properties when exposed to humid air: When equilibrated at room temperature for several days in a relative humidity of approximately 97.3%, the material turned into a brittle solid. We used a multi-method approach in order to characterize this starch material and to investigate hydration- and temperature-driven phase transitions.

### 3.1. Scanning electron microscopy

Scanning electron microscopy was used to characterize the acid hydrolyzed starch granules. For the sake of comparison, both native and acid hydrolyzed starches were observed. To minimize the influence of moisture, vacuum conditions were used. As shown in Fig. 1, the micrographs revealed major differences in shape, surface roughness, and size distribution between the two materials. Native potato starch granules are smooth and oval with long-axis lengths between 15 and 75 µm. In contrast, the acid hydrolyzed starch appears in the form of wrinkled spheres with multiple cracks and holes on the surface. As Fig. 1 shows, there is a significant difference in the size distribution, which for the acid-treated material is broader with diameters between 5 and 120 µm. The acid hydrolyzed starch was also examined at different levels of water activity. The micrographs taken at different relative humidities showed a gradual swelling and disruption of the granules (Supplementary Material, Figure S2).

### 3.2. Sorption calorimetry

In order to investigate the nature of the aforementioned hydration-driven physical transition, we investigated the starch by means of sorption calorimetry which, in one experiment, gives the sorption isotherm and the partial molar enthalpy of mixing of water (hydration enthalpy). Completely dry starch was loaded into the sorption calorimeter cell under a dry atmosphere and the water activity was subsequently continuously slowly increased. In a second experiment, starch, which was first exposed for 1 week to a relative humidity of approximately 97.3% (in the presence of a saturated $K_2SO_4$ solution) at room temperature and subsequently dried in vacuum and ground in a mortar, was investigated. The resulting sorption isotherms and hydration enthalpy curves are shown in Fig. 2.

In Fig. 2(a) we note that the two sorption isotherms are strikingly different: while the moisture exposed material shows no sudden events upon hydration, the spray-dried material displays a step in $a_w$ at a water concentration of approximately 21.5 wt%. This is indicative of a phase transition. At low water activities, the spray-dried material takes up more water than the moisture-exposed material, which suggests that the former is in a less ordered state. At water activities between approximately 0.37 and 0.59 as well as for water activities above approximately 0.96, the sorption isotherms essentially coincide.

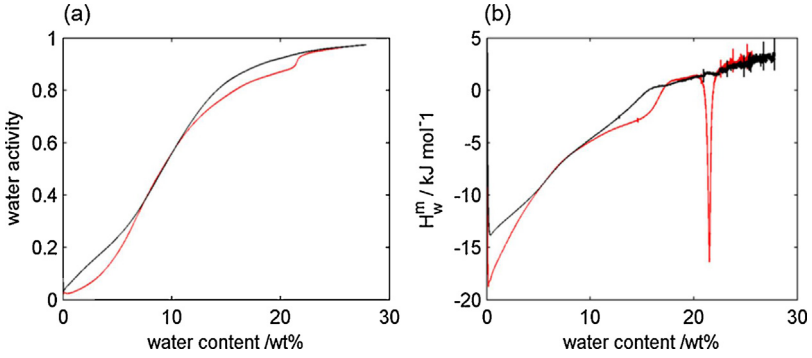


**Fig. 2.** Sorption isotherms (a) and enthalpies of hydration (b) for untreated spray-dried acid hydrolyzed starch (red curves) and the same material recrystallized prior hydration (black curves). Both experiments were performed at 25 °C. (For interpretation of the references to color in this figure legend, the reader is referred to the web version of the article.)

Like the sorption isotherms, the hydration enthalpy curves for the two differently pretreated materials also show large differences, see Fig. 2(b). The moisture-exposed material shows a kink at approximately 15 wt% of water. The spray-dried material has a large endothermic step at 16.5 wt% of water and a sharp exothermic peak at 21.5 wt% of water; the former indicates a glass transition whereas the latter indicates a phase transition. It should be noted that the exothermic event observed in the hydration enthalpy plot coincides with the step found in the corresponding sorption isotherm. The lack of an endothermic step (glass transition) in the pre-hydrated material suggests that it is predominantly in a crystalline state. It should be noted that the enthalpy of hydration at zero water content for the untreated material but not for the pre-hydrated is close to $-18$ kJ mol$^{-1}$, a value found for several biopolymers (Kocherbitov, Arnebrant, & Soderman, 2004; Kocherbitov, Ulvenlund, Briggner, Kober, & Arnebrant, 2010; Kocherbitov, Ulvenlund, Kober, Jarring, & Arnebrant, 2008; Znamenskaya, Sotres, Engblom, Arnebrant, & Kocherbitov, 2012).

For the spray-dried starch, another experiment was performed at 40 °C (Supplementary Material, Figure S3). Qualitatively, the results were very similar to those recorded at 25 °C; however, comparison of the sorption isotherms and hydration enthalpy curves obtained at different temperatures reveals that both the glass transition and the exothermic event occurred at slightly lower water contents at the elevated temperature. Thus, the glass transition occurred at 15.5 wt% of water at 40 °C (16.5 wt% at 25 °C) and the exothermic event occurred at 19.2 wt% of water at 40 °C (21.5 wt% at 25 °C). Apart from the position of the step, the sorption isotherms recorded at 25 °C and 40 °C were almost identical at water activities below 0.85 and above 0.95.

### 3.3. Quartz crystal microbalance with dissipation monitoring

While sorption calorimetry gives information on the bulk properties of a material, quartz crystal microbalance with dissipation monitoring (QCM-D) may be used to obtain data for thin films (Fogel & Limson, 2011; Lubarsky, Davidson, & Bradley, 2007; Znamenskaya et al., 2012). Due to its high sensitivity, this technique delivers real-time analysis of the thickness, swelling, and rheological properties of the sample. We used a newly developed humidity scanning QCM-D method (Graf & Kocherbitov, 2013) to investigate starch films of various thicknesses which were prepared by drop-coating the sensor with dilute aqueous solutions of acid hydrolyzed starch. As Fig. 3(a) shows, the sorption isotherms obtained with the QCM-D method are in close agreement with the sorption calorimetry data.

Strikingly, in the sorption isotherms recorded with the QCM-D method we also observe the step that we previously found in sorption calorimetry and related to a crystallization phase transition. The water activity at which the step appears is in close agreement with the calorimetric data. The small differences in sorption isotherms that the two methods produce could be resulting from the fact that sorption calorimetry measures bulk properties whereas QCM-D examines thin films, and so consequently the diffusion rates within the materials as well as the equilibration times should be different. Also, crystallization during preparation of the sample for QCM-D experiments plays a role. As Fig. 3(b) shows, the dissipation is close to 0 until the water activity reaches around 0.85; at this point an increase is noted. Such a behavior corresponds to a transition from a rigid into a flexible state which can be ascribed to the glass transition of the material. At even higher water activity, ca 0.93, we observe a peak. As discussed in the sorption

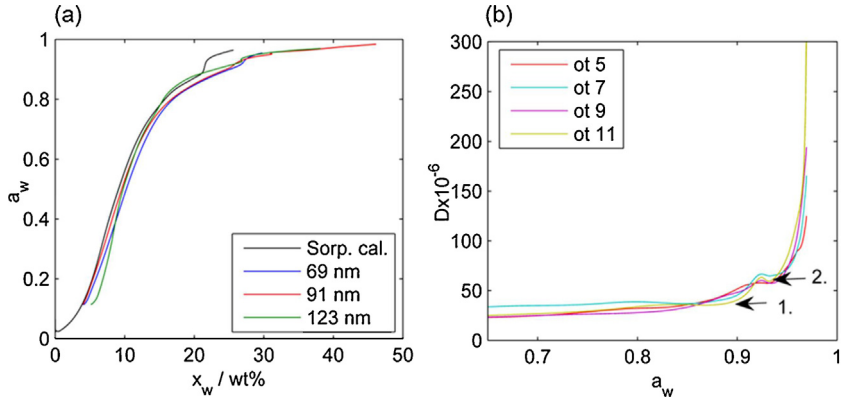


**Fig. 3.** Sorption isotherms obtained by QCM-D for different film thicknesses in comparison to sorption calorimetric data (a), and the water activity-dissipation dependence for selected overtones for the 123 nm thick starch film (b). The arrows point at events corresponding to glass transition (1) and crystallization (2).

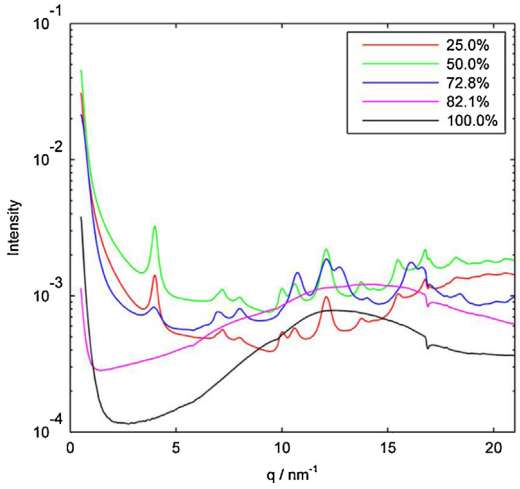


**Fig. 4.** WAXS spectra (intensity vs. the scattering vector, $q$) of acid hydrolyzed starch at different starch concentrations. The legend shows the starch content in wt%.

calorimetry section above, this event is related to crystallization of the starch.

It is important to point out that the QCM-D samples were suspended in water prior to measurement as the sensor was drop-coated. Surprisingly, the results are comparable to those from sorption calorimetry which indicate that the film is to a large extent in an amorphous state in the beginning of the QCM-D experiment. This shows that, despite exposure to high water activity during coating of the QCM-D sensor, the sample does not undergo complete crystallization. The reason is probably in the time of equilibration, since the suspension was prepared directly before covering the sensor. Also, effects of the presence of the solid surface of the sensor may play a role. Later, during the scanning experiment that takes several hours the equilibrium is being slowly achieved and the remaining amorphous part of the sample undergoes further crystallization.

### 3.4. Wide-angle X-ray scattering

In order to investigate the structural changes of the starch as a function of hydration, samples in a broad composition range were prepared and analyzed with wide-angle X-ray scattering (WAXS). The results are shown in Fig. 4. No Bragg reflections were found in samples with water contents below 17.9 wt%; this indicates a lack of molecular order, i.e., the amorphous state of the material. Samples with higher water content show several distinct Bragg reflections indicating crystalline ordering. It should be noted that the Bragg reflections from the samples containing 25 and 50 wt% of starch are in good agreement while the Bragg reflections for the sample containing 72.8 wt% (equilibrated in the presence of a saturated $K_2SO_4$ solution) of starch are partially different.

The WAXS spectrum of 25 wt% of acid hydrolyzed starch was compared to that of native potato starch at the same concentration (Supplementary Material, Figure S4). It was found that the Bragg reflection patterns for the two materials were almost identical, which indicates the same type of structure, i.e., the B type crystallinity typically found in tuber starches. However, it should be noted that while the 9 nm lamellar peak is present in native potato starch it is absent in the acid-treated material. The B type symmetry was confirmed by detailed analysis of the peak positions. Comparison to literature data suggest that all Bragg reflections obtained for 25 and 50 wt% match the hexagonal unit cell created by the left-handed double helixes of starch which correspond to the B type crystallinity ($a = b = 1.85$ nm, $c = 1.04$ nm, $P6_1$ space group) (Hsein-Chih & Sarko, 1978a; Imberty & Pérez, 1988).

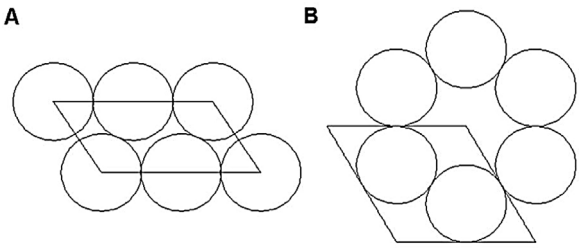


**Fig. 5.** Schematic representations of A and B type crystalline structures.

As noted above, the sample containing 72.8 wt% of acid hydrolyzed starch shows a different Bragg reflection pattern. Analysis of the peak positions shows that only a part of the peaks originates from the B type crystallites. The additional reflections, occurring at $q$ values of 10.8, 12.8, and 16.4 $nm^{-1}$, are instead characteristic for the A type crystallinity pattern (Cardoso & Westfahl, 2010; Cheetham & Tao, 1998). Since we clearly observe reflections from both structures we can conclude that A and B type crystallites coexist in this sample. Such an allomorph is sometimes referred to as C type starch (Cardoso & Westfahl, 2010; Cheetham & Tao, 1998). Schematic representations of A and B type crystallites are found in Fig. 5.

The type of crystallinity expressed in certain plant species strongly depends on the length of the short chain fraction in amylopectin (the chain fragments between the branching points). Two starch helixes can associate as soon as their degree of polymerization exceeds nine. Above DP of 10, the duplexes can form crystals. On average shorter chains (DP 10–12) form A type crystallites whereas longer form B type (>12 DP) (Imberty, Buléon, Tran, & Pérez, 1991; Tester, Karkalas, & Qi, 2004). Another factor is the incorporation of water. To form B structure both long enough chains and a sufficient number of water molecules are required (Cleven, van Den Berg, & van der Plas, 1978). As discussed above, in the acid hydrolyzed starch hydration induces an ordered structure. At low water content, the helixes are packed in tight monoclinic A type crystallites. With increased moisture content the B type is formed, because there are a sufficient number of water molecules to fill the central cavity of its hexagonal structure. That reflects the general rule that A type starch appears in plants growing in warm and dry conditions (e.g., in cereal grain), whereas the B type is found in wet and cold environment (e.g., in potato tuber) (Buléon et al., 1998; Pérez & Bertoft, 2010).

### 3.5. Small-angle X-ray scattering

Small-angle X-ray scattering was used to determine structural changes resulting from hydration or thermal processing of either amorphous or recrystallized acid hydrolyzed starch.

We distinguished four different patterns in the SAXS spectra for samples in the range of 25–100 wt% of the initially amorphous starch, see Fig. 6(a). Bragg reflections appear for the three lowest starch concentrations: 25.0, 50.0 and 72.8 wt%. However, the latter differs in shape which, as indicated in the WAXS discussion, is due to the presence of a different crystalline structure in this material. The positions of the peaks in SAXS are the same as for the corresponding peaks in WAXS. In all samples with a starch concentration above 82.1 wt%, no Bragg reflections are present; however, there is a pronounced difference between the results for 82.1 wt% of starch and those obtained for higher starch concentrations. We suggest that the reason for these differences is the occurrence of the glass transition between 82.1 and 85.9 wt% at room temperature. Indeed, according to the sorption calorimetric data, at 25 °C the glass transition is at 16.5 wt% of water, i.e., 83.5 wt% of starch. Furthermore, all of the samples were examined

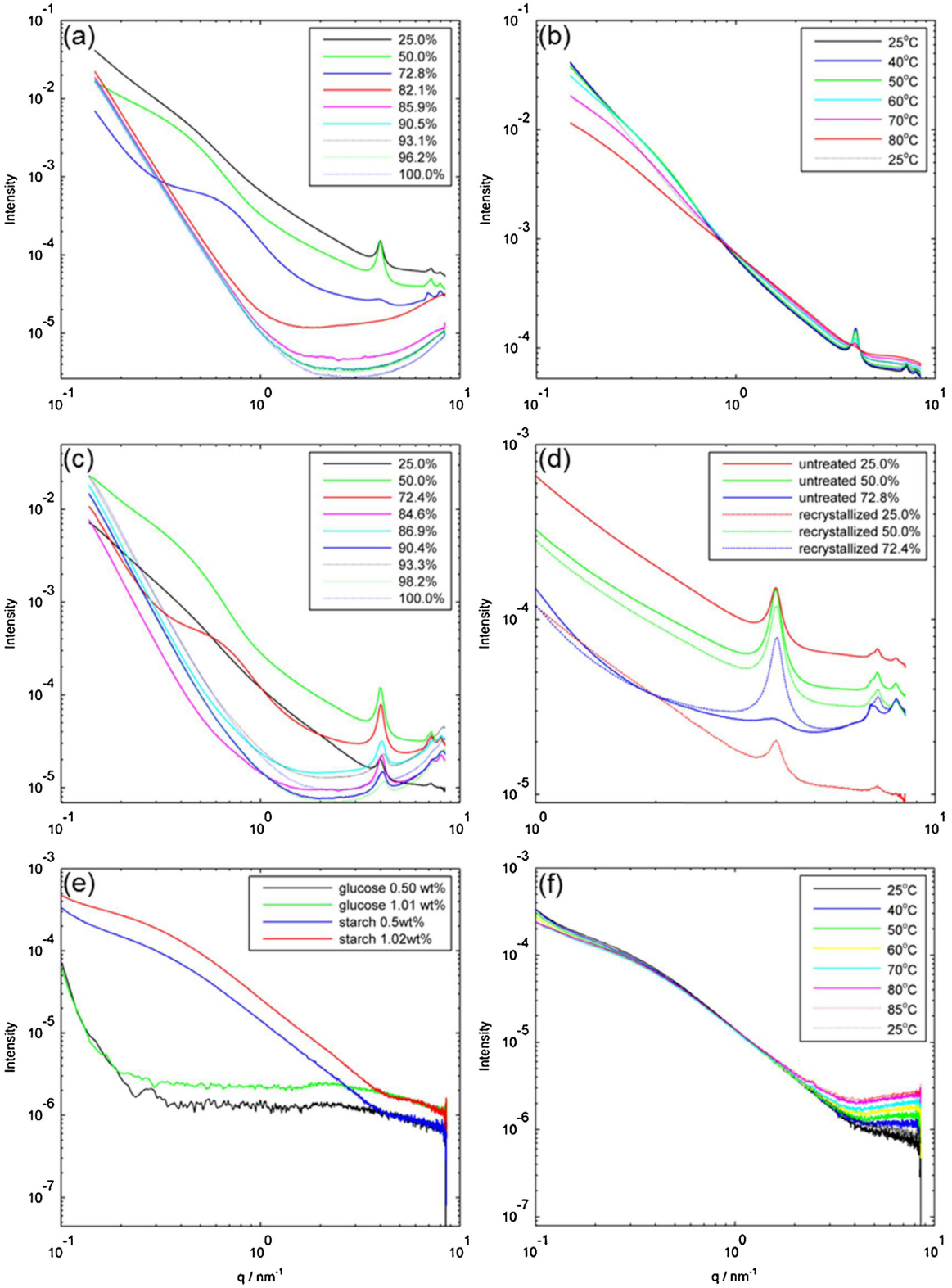


**Fig. 6.** Comparison of SAXS patterns for different concentrations at 25 °C (a) and for a sample of 25 wt% of starch at different temperatures (b). The Bragg reflections for samples of various concentrations of recrystallized acid hydrolyzed starch at 25 °C (c) and comparison of its positions for the untreated and recrystallized starch (d). Comparison of SAXS for dilute acid hydrolyzed starch and glucose at concentrations of 0.5 and 1% (e) and a temperature scan for a sample of 0.5% of acid hydrolyzed starch (f).

at several temperatures ranging from 25 to 80 °C. As an example, in Fig. 6(b) temperature scans for 25 wt% of starch are presented. All of those showed decreased intensity of the Bragg reflections with increased temperature. In SAXS data for several compositions at 80 °C, we note that the glass transition occurs in the same interval as that found at 25 °C (Supplementary Material, Figure S5).

Analysis of the peak area as a function of temperature revealed that for 25 and 50 wt% of starch, all of the peaks decay with

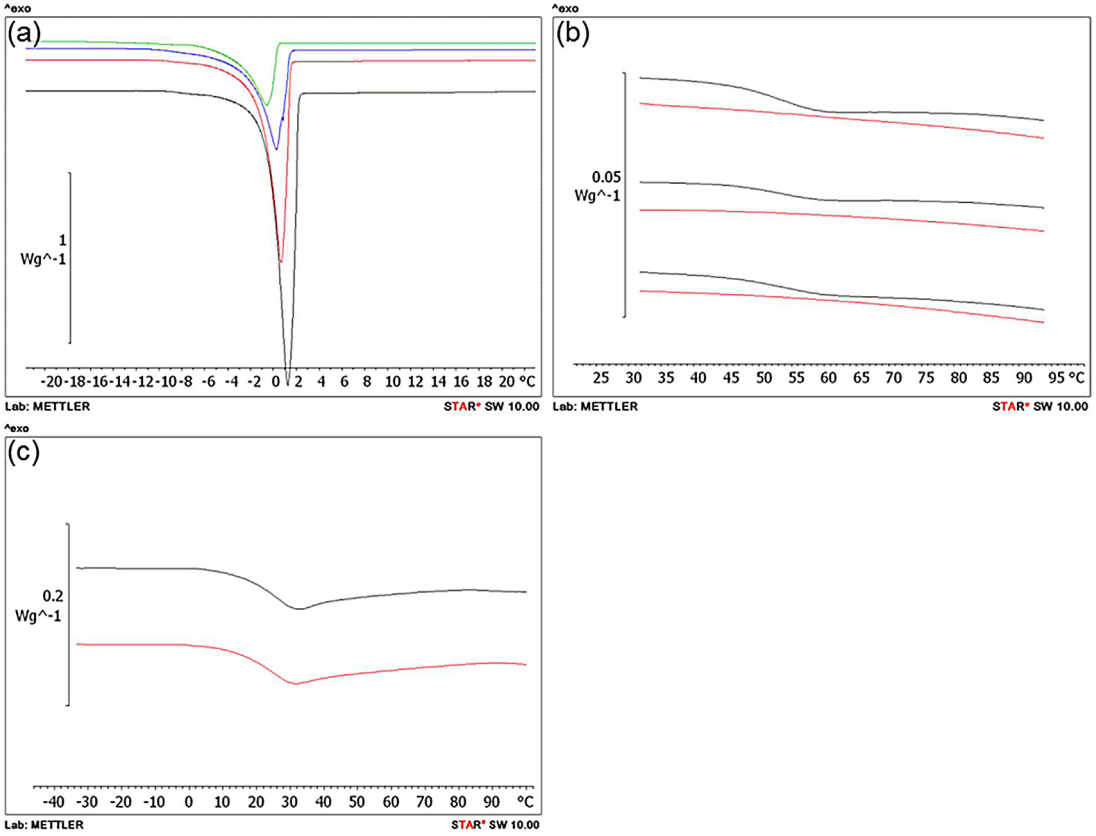


**Fig. 7.** DSC thermograms for selected compositions showing the water melting peak for samples (in order from the top) of 25, 40, 50, 60 wt% of starch (a), gelatinization peak both first (black) and second (red) scans for 62.6, 68.7, and 71.2 wt% of starch (b), and the glass transition found in the first (black) and second (red) scans for 82.1 wt% of starch (c). (For interpretation of the references to color in this figure legend, the reader is referred to the web version of the article.)

sigmoidal dependence, with the midpoint around 59 °C (Supplementary Material, Figure S6). However, the behavior of the sample containing both A and B type crystallites is slightly different. We observe that the first peak ($q$ equal to 4.0 $nm^{-1}$) characteristic for the B type pattern decays as in the other samples while the following peaks are less affected. The decreased intensities of the reflections most probably correspond to a gradual disruption of the crystalline structure. These results suggest that the A type crystallites are disrupted at higher temperature than the B type structure.

Recrystallized samples, regardless of the level of hydration, showed three Bragg reflections in the SAXS spectrum which suggest that the hydration-induced crystallites are stable upon drying, see Fig. 6(c). A comparison of the SAXS patterns for the untreated and the recrystallized materials is presented in Fig. 6(d). We note a slight change of the peak positions to lower $q$ values for the recrystallized starch with increased hydration. We link this observation to the fact that the helixes within the crystallites contract during drying and then swell upon hydration as water fills the voids. Heating the recrystallized samples leads to decreased peak intensities as the structure is disrupted; however, all of the samples except that corresponding to 25 wt% of starch retain the main peak ($q = 4\ nm^{-1}$) in the studied temperature range (Supplementary Material, Figure S7). SAXS measurements were also performed for solutions of 0.5 and 1 wt% of starch as well as for the same concentrations of glucose. As presented in Fig. 6(e), the plots partially coincide indicating that in the high $q$ range the signal comes from individual glucose units within the starch molecule. When heated the intensity at high $q$ values increases, probably as a result of shifts in the glucose conformation, see Fig. 6(f). Finally, three regimes can be distinguished in the SAXS plots for dilute starch samples (Supplementary Material, Figure S8). The shape of the middle part of the curve in the range of $q$ values of 0.4–3 $nm^{-1}$ is dependent on the polymer chain conformation in the solution. From the slope of the linear part of the curve, the value of the Flory exponent for acid hydrolyzed starch was calculated to be to 0.53.

### 3.6. Differential scanning calorimetry

We used differential scanning calorimetry (DSC) in order to investigate thermal events of the starch–water system. Results for a few selected sample compositions are shown in Fig. 7. From the enthalpy of melting of water we determined the amount of nonfreezing water in acid hydrolyzed starch to be 0.34 g/g (corresponding to an average of 3.0 water molecules for each repeating unit of starch, Supplementary Material, Figure S9) while for native starch the value was found to be 0.36 g/g (3.2 water molecules for each repeating unit). The lower value for acid hydrolyzed starch may be interpreted as a difference in the crystalline fraction between the two materials (it should be noted that native potato starch comprises a significant amorphous fraction).

A broad endothermic event was found; it should be noted that this event showed up in the first scan but not in a second scan performed directly after the first, Fig. 7(b). However, upon storage for several days this event reappeared. The event may be attributed to crystalline melting and unwinding of the helixes upon thermal treatment (gelatinization). The reappearance of the peak might thus be attributed to restoring of the structure upon time (retrogradation). Furthermore, it was noticed that the DSC scan rate affected the shape and position of the peak. In particular, the transition occurred at slightly higher temperatures for higher scan rates, which indicates that a kinetic contribution plays a role.

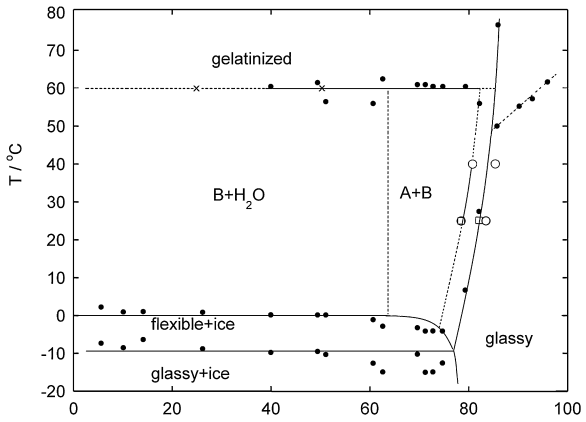


**Fig. 8.** Phase diagram of the acid hydrolyzed starch–water system. Symbols: (□) stands for QCM-D, (●) for DSC, (○) for sorption calorimetry data, x for SAXS data. The dashed line in the right upper corner corresponds to the sub-$T_g$ event.

For starch concentrations up to ca. 77 wt% the glass transitions occurred at temperatures below ice melting. Above this concentration the glass transition temperature increases rapidly as the water content decreases. An example of glass transition found with DSC is presented in Fig. 7(c). For amorphous samples we found what has been referred to as a sub-$T_g$ endotherm (Thiewes & Steeneken, 1997). The temperature at which this event occurred increased slightly with decreasing water content.

### 3.7. Phase diagram

Taken together, the information obtained from all methods was used to construct a phase diagram, which is shown in Fig. 8 and can be compared to the one for native starch found in the literature (van der Sman & Meinders, 2011). To the best of our knowledge, this is the first phase diagram presented for acid hydrolyzed starch–water. The melting of ice was found as an endothermic peak in DSC. The glass transition was observed in several methods as described above and it separates regions containing glassy and rubbery/flexible starch. Above the glass transition the polymer can rearrange which allows crystallization. This event was observed both in sorption calorimetry and QCM-D measurements and the type of crystallinity was determined by WAXS. With increasing temperature the crystalline structure is disrupted, which is a process included in the gelatinization phenomenon. The gelatinization line was drawn based on the DSC result as well as on the evaluation of the decay of the peaks found in SAXS.

As it was shown that depending on moisture content different types of crystallinity are expressed, we deduce that there should be another phase border that ideally would correspond to pure B type starch. In reality, probably neither A or B structures are fully crystalline, therefore the phase boundary shown as a vertical dashed line is approximate and can be dependent on the history of sample.

## 4. Conclusions

Employing a multi-method approach, we have examined the physical properties of spray-dried acid hydrolyzed potato starch (maltodextrin) upon hydration and found that:

- The dry material is, initially, in an amorphous, glassy state.
- The glass transition at 25 °C occurs at a water content of 16.5 wt%, and at a water content of 21.5 wt% the flexible starch crystallizes.
- The sorption isotherms and hydration enthalpy plots for the amorphous and recrystallized dried materials are strikingly different indicating the influence of non-equilibrium effects in the system.
- Glass transition and crystallization were found in both bulk samples and thin films.
- The presence and type of crystallinity expressed by the starch is strongly related to the hydration level; thus A and B type crystallites coexist at low hydration levels whereas only B crystallites are present at higher water contents.
- The crystalline structures are gradually destroyed at elevated temperatures; however, the A type crystallites appear to be less sensitive to temperature than the B type crystallites.
- The amount of nonfreezing water was found to be 0.34 g/g (3.0 water molecules per repeating unit of starch). This value is lower than that for native potato starch and thus indicates a more ordered system.

Our findings were used to construct the first phase diagram of acid hydrolyzed starch–water, and illustrate principles of hydration-induced phenomena in biopolymers.

## Acknowledgements

We thank the MAX IV Laboratory for the opportunity to perform SAXS and WAXS experiments and we are especially grateful to Tomás S. Plivelic and Sylvio Haas. Financial support from Knowledge Foundation (KK-stiftelsen, grant number 20110158), from Biofilms Research Center for Biointerfaces and from Gustav Th Ohlsson Foundation is gratefully acknowledged.

## Appendix A. Supplementary data

Supplementary data associated with this article can be found, in the online version, at http://dx.doi.org/10.1016/j.carbpol.2014.06.037.

## References

Buléon, A., Colonna, P., Planchot, V., & Ball, S. (1998). Starch granules: Structure and biosynthesis. *International Journal of Biological Macromolecules*, *23*, 85–112.
Cardoso, M. B., & Westfahl, H., Jr. (2010). On the lamellar width distributions of starch. *Carbohydrate Polymers*, *81*, 21–28.
Cheetham, N. W. H., & Tao, L. (1998). Variation in crystalline type with amylose content in maize starch granules: An X-ray powder diffraction study. *Carbohydrate Polymers*, *36*, 277–284.
Cleven, R., van Den Berg, C., & van der Plas, L. (1978). Crystal structure of hydrated potato starch. *Starch/Staerke*, *30*, 223–228.
Donovan, J. W. (1979). Phase transitions of the starch–water system. *Biopolymers*, *18*, 263–275.
Fogel, R., & Limson, J. L. (2011). Probing fundamental film parameters of immobilized enzymes—Towards enhanced biosensor performance Part I—QCM-D mass and rheological measurements. *Enzyme and Microbial Technology*, *49*, 146–152.
French, D. (1972). Fine structure of starch and its relationship to the organization of starch granules. *Journal of the Japanese Society of Starch Science*, *19*, 8–25.
Graf, G., & Kocherbitov, V. (2013). Determination of sorption isotherm and rheological properties of lysozyme using a high-resolution humidity scanning QCM-D technique. *The Journal of Physical Chemistry B*, *117*, 10017.
Greenspan, L. (1976). Humidity fixed points of binary saturated aqueous solutions. *Journal of Research of the National Bureau of Standards*, *81A*, 89–96.
Hammersley, A. (1997). FIT2D: An introduction and overview. In *ESRF Internal Report ESRF97HA02T*.
Hsein-Chih, H. W., & Sarko, A. (1978). The double-helical molecular structure of crystalline b-amylose. *Carbohydrate Research*, *61*, 7–25.
Hsien-Chih, H. W., & Sarko, A. (1978). The double-helical molecular structure of crystalline a-amylose. *Carbohydrate Research*, *61*, 27–40.
Imberty, A., Buléon, A., Tran, V., & Pérez, S. (1991). Recent advances in knowledge of starch structure. *Starch/Staerke*, *43*, 375–384.
Imberty, A., & Pérez, S. (1988). A revisit to the three-dimensional structure of B-type starch. *Biopolymers*, *27*.
Jenkins, P. J., & Donald, A. M. (1998). Gelatinisation of starch: A combined SAXS/WAXS/DSC and SANS study. *Carbohydrate Research*, *308*, 133–147.
Johannsmann, D. (1999). Viscoelastic analysis of organic thin films on quartz resonators. *Macromolecular Chemistry and Physics*, *200*, 501–516.
Karapantsios, T. D., Sakonidou, E. P., & Raphaelides, S. N. (2002). Water dispersion kinetics during starch gelatinization. *Carbohydrate Polymers*, *49*, 479–490.
Karlsson, M. E., & Eliasson, A. (2003). Gelatinization and retrogradation of potato (*Solanum tuberosum*) starch in situ as assessed by differential scanning calorimetry (DSC). *LWT-Food Science and Technology*, *36*, 735–741.

Knill, C. J., & Kennedy, J. F. (2005). In S. Dumitriu (Ed.), *Polysaccharides. Structural diversity and functional versatility* (p. 605). New York: Marcel Dekker.
Kocherbitov, V., Arnebrant, T., & Soderman, O. (2004). Lysozyme–water interactions studied by sorption calorimetry. *The Journal of Physical Chemistry B*, *108*, 19036–19042.
Kocherbitov, V., Ulvenlund, S., Kober, M., Jarring, K., & Arnebrant, T. (2008). Hydration of microcrystalline cellulose and milled cellulose studied by sorption calorimetry. *The Journal of Physical Chemistry B*, *112*, 3728–3734.
Kocherbitov, V. (2004). A new formula for accurate calculation of water activity in sorption calorimetric experiments. *Thermochimica Acta*, *414*, 43–45.
Kocherbitov, V., Ulvenlund, S., Briggner, L., Kober, M., & Arnebrant, T. (2010). Hydration of a natural polyelectrolyte xanthan gum: Comparison with non-ionic carbohydrates. *Carbohydrate Polymers*, *82*, 284–290.
Labrador, A., Cerenius, Y., Svensson, C., Theodor, K., & Plivelic, T. (2013). The yellow mini-hutch for SAXS experiments at MAX IV laboratory. *Journal of Physics: Conference Series*, *425*, 072019.
Lelièvre, J., & Liu, H. (1994). A review of thermal analysis studies of starch gelatinization. *Thermochimica Acta*, *246*, 309–315.
Lin, N., Huang, J., Chang, P. R., Anderson, D. P., & Yu, J. (2011). Preparation, modification, and application of starch nanocrystals in nanomaterials: A review. *Journal of Nanomaterials*, 13.
Lourdin, D., Coignard, L., Bizot, H., & Colonna, P. (1997). Influence of equilibrium relative humidity and plasticizer concentration on the water content and glass transition of starch materials. *Polymer*, *38*, 5401–5406.
Lubarsky, G. V., Davidson, M. R., & Bradley, R. H. (2007). Hydration–dehydration of adsorbed protein films studied by AFM and QCM-D. *Biosensors and Bioelectronics*, *22*, 1275–1281.
Morikawa, K., & Nishinari, K. (2000). Rheological and DSC studies of gelatinization of chemically modified starch heated at various temperatures. *Carbohydrate Polymers*, *43*, 241–247.
Pérez, S., & Bertoft, E. (2010). The molecular structures of starch components and their contribution to the architecture of starch granules: A comprehensive review. *Starch/Staerke*, *62*, 389–420.
Sauerbrey, G. (1959). Verwendung Von Schwingquarzen Zur Wägung Dünner Schichten Und Zur Mikrowägung. *Zeitschrift Fur Physik A-Hadrons and Nuclei*, *1555*, 206–222.
Tester, R. F., Karkalas, J., & Qi, X. (2004). Starch—Composition, fine structure and architecture. *Journal of Cereal Science*, *39*, 151–165.
Thiewes, H. J., & Steeneken, P. A. M. (1997). The glass transition and the sub-Tg endotherm of amorphous and native potato starch at low moisture content. *Carbohydrate Polymers*, *32*, 123–130.
van der Sman, R. G. M., & Meinders, M. B. J. (2011). Prediction of the state diagram of starch water mixtures using the Flory-Huggins free volume theory. *Soft Matter*, *7*, 429.
Vermeylen, R., Derycke, V., Delcour, J. A., Goderis, B., Reynaers, H., & Koch, M. H. (2006). Structural transformations during gelatinization of starches in limited water: Combined wide- and small-angle X-ray scattering study. *Biomacromolecules*, *7*, 1231–1238.
Vermeylen, R., Derycke, V., Delcour, J. A., Goderis, B., Reynaers, H., & Koch, M. H. J. (2006). Gelatinization of starch in excess water: Beyond the melting of lamellar crystallites. A combined wide- and small-angle X-ray scattering study. *Biomacromolecules*, *7*, 2624–2630.
Wadsö, I., & Wadsö, L. (1996). A new method for determination of vapour sorption isotherms using a twin double microcalorimeter. *Thermochimica Acta*, *271*, 179–187.
Wadsö, L., & Markova, N. (2002). A method to simultaneously determine sorption isotherms and sorption enthalpies with a double twin microcalorimeter. *Review of Scientific Instruments*, *73*, 2743–2754.
Waigh, T. A., Gidley, M. J., Komanshek, B. U., & Donald, A. M. (2000). The phase transformations in starch during gelatinisation: A liquid crystalline approach. *Carbohydrate Research*, *328*, 165–176.
Znamenskaya, Y., Sotres, J., Engblom, J., Arnebrant, T., & Kocherbitov, V. (2012). Effect of hydration on structural and thermodynamic properties of pig gastric and bovine submaxillary gland mucins. *The Journal of Physical Chemistry B*, *116*, 5047–5055.